Inelastic neutron scattering study of tetramethylpyrazine in the complex with chloranilic acid

2005 J. Phys.: Condens. Matter 17 5725

(http://iopscience.iop.org/0953-8984/17/37/010)

INSTITUTE OF PHYSICS PUBLISHING JOURNAL OF PHYSICS: CONDENSED MATTER

J. Phys.: Condens. Matter **17** (2005) 5725–5739 doi:10.1088/0953-8984/17/37/010

Inelastic neutron scattering study of tetramethylpyrazine in the complex with chloranilic acid

M Prager[1], A Pawlukojc[2], L Sobczyk[3], E Grech[4] and H Grimm[1]

[1] Institut für Festkörperforschung, Forschungzzentrum Jülich, D-52425 Jülich, Germany
[2] Institut of Nuclear Chemistry and Technology, Warsaw, Poland
[3] Faculty of Chemistry, University of Wroclaw, Poland
[4] Institute of Chemistry, Szczecin University of Technology, Poland

Received 14 May 2005, in final form 4 August 2005
Published 2 September 2005
Online at stacks.iop.org/JPhysCM/17/5725

Abstract

The tunnel splitting of the methyl librational ground states in the hydrogen bonded tetramethylpyrazine–chloranilic acid (TMP–CLA) complex are determined for temperatures $T \leqslant 28$ K by high resolution neutron spectroscopy. Three tunnel modes are resolved at $T = 2.4$ K. Their relative intensities show that the crystal structure must be different from the proposed space group. Tunnelling and methyl librational modes from the measured density of states are combined into rotational potentials. There are discrepancies of activation energies calculated for these potentials and those obtained from quasielastic scattering of neutrons at $T \geqslant 50$ K due to structural differences in the two respective temperature regimes. Rotational potentials in TMP–CLA are significantly weaker as in pure TMP.

(Some figures in this article are in colour only in the electronic version)

1. Introduction

As shown in the reviews [1, 2] the tunnel splitting of rotating groups such as CH_3 or NH_3 can yield important information on the interaction effects of both inter- and intramolecular origin, via their rotational potential. The magnitude of the tunnel splitting is strictly correlated with the potential shape and can be recorded by high resolution inelastic neutron spectroscopy (INS). Like classical lattice dynamics rotational potentials can be calculated on the basis of a precise crystal structure and intermolecular interaction potentials. Due to its exponential dependence on the height of the rotational barrier rotational tunnelling spectroscopy is one of the most sensitive methods to test or/and improve atom–atom potentials [3, 4]. For this reason we attempt to use the tunnel splitting in studies of systems with specific interactions, such as charge-transfer and hydrogen bonding. A sufficient tendency towards such interaction can

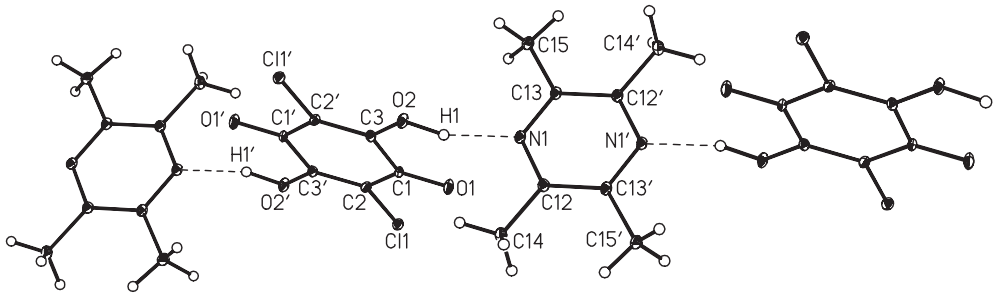

Figure 1. Building unit of the TMP–CLA 1:1 complex as derived from x-ray diffraction at $T = 100$ K [10]. Due to an inversion centre the irreducible units are half of each molecule. O–H $\cdots$ N bonds along **a**-, stacking along **b**-axis.

lead in binary alloys to the formation of stoichiometrically defined complexes with interesting, sometimes new, properties.

A typical electron donor in such complexes is 1,2,4,5-tetramethylbenzene, durene. This material was recently successfully studied by neutron spectroscopy [5, 6]. While high energy internal modes above $\sim$300 cm^{-1} are well described by quantum chemistry models (GAUSSIAN98), modes at low frequency ascribed to rotation and deformation of CH_3 groups substantially depend on the environment. A similar result is obtained for a large number of other systems systematically analysed in [7]. Thus, low frequency modes can give the clearest information on specific intermolecular interactions.

We started the search for a suited system with complexes formed by tetramethylpyrazine (TMP). TMP was chosen since symmetry of the molecule is identical to that of durene. Furthermore, the crystal structure or pure TMP is known [8, 9]. Finally, the ability to form complexes being both π- and n-electron donors makes TMP mixable with a large number of counter-molecules. As the counterpart in the complex chloranilic acid (CLA) was chosen, which shows both proton-donor and π-electron-acceptor properties, and which was shown recently [10] to form relatively simple 1:1 hydrogen bonded complexes with TMP.

The crystal structure of the complex was studied by x-rays. Above $T = 100$ K the crystalline lattice consists of infinite chains along the a axis with strong hydrogen bonds (figure 1), while the TMP and CLA rings are stacked along the b axis (monoclinic, space group $P2_1/c$). In the packing a decisive role is played by hydrogen bond interactions. In addition to the main O–H $\cdots$ N bridges (without proton transfer), unconventional C–H $\cdots$ O and C–H $\cdots$ Cl hydrogen bonds are present, which are expected to affect the dynamical behaviour of CH_3 groups.

Besides the fundamental question of the special intermolecular interaction of TMP–CLA dimers which leaves its fingerprint in the CH_3 group dynamics the complexes of CLA seem to be interesting from the point of view of materials science. Thus, as pointed out, CLA can be treated as a component of supramolecular synthons in crystal engineering [11] and, belonging to the benzoquinones, is interesting from the point of view of the electron transfer processes including biological systems [12, 13]. But most interesting seem to be the complexes of CLA with nitrogen bases such as pyridine and diazines [14] pyrazole and imidazole [15] and, above all, pyrimidine and pyrazine [16].

The present work uses the technique of INS to obtain the characteristic excitation energies via the scattering function $S(Q, \omega)$ from 1 μeV to $\sim$100 meV. Tunnel splittings observed at temperatures $T \leqslant 36$ K, activation energies deduced from quasielastic scattering of methyl groups at sample temperatures up to $T = 120$ K and methyl torsional vibrations identified

in the spectra of lattice phonons are consistently described by rotational potentials. Other external and internal modes are also assigned in the data analysis. The clarification of the phase diagram and refinements of TMP–CLA crystal structures for future use in mathematical modelling is a problem of its own and beyond the scope of the present work.

2. Theory

The standard description of rotational tunnelling and quasielastic scattering is the single-particle model (SPM) [1]. SPM represents a mean field theory. The environment of the molecule is represented by a rotational potential $V(\varphi)$. Due to the symmetry of the methyl group it is expressed in the form of a Fourier expansion of threefold symmetry up to order J

$$V(\varphi) = \sum_{j=1}^{J} \frac{V_{3j}}{2}(1 - \cos(3j\varphi - \varphi_{3j})). \tag{1}$$

At low temperatures when the classical rotational jump dynamics is frozen this potential determines the excitations of the hindered quantum rotor by the eigenvalues E_i of the stationary single-particle Schrödinger equation [1, 2]

$$\left\{-B\frac{\partial^2}{\partial\varphi^2} + V(\varphi)\right\}\Psi_i = E_i\Psi_i. \tag{2}$$

Here $B = \frac{\hbar^2}{2\Theta} = 0.655$ meV is the rotational constant of the methyl group with the moment of inertia Θ. The tunnel splitting is the difference between the two lowest levels $\hbar\omega_t = E_1 - E_0$. The knowledge of further transitions to higher rotational states, $E_j - E_i$, must be known if the shape of the rotational potential is to be refined.

High resolution neutron spectroscopy is an especially successful technique to observe the low energy transitions of weakly hindered rotors. In particular, the ground-state tunnel splitting $\hbar\omega_t$ gives rise to a simple scattering function [1, 2]. In the present example we consider $N = 4$ inequivalent methyl groups of occurrence probabilities $p(n)$ in TMP and $M = 2$ individual protons in the CLA molecule which scatter only elastically, and obtain the scattering function

$$S(Q,\omega) = (\tfrac{5}{3}+\tfrac{4}{3}j_0(Qd)) + (M/N)\delta(\omega) + \sum_{n=1}^{N} p(n)(\tfrac{2}{3} - \tfrac{2}{3}j_0(Qd))\{\delta(\omega+\omega_{t_n}) + \delta(\omega-\omega_{t_n})\} \tag{3}$$

with momentum transfer Q and distance d of the protons in the methyl group. For fully resolved tunnelling bands the theory yields a ratio $\frac{I_{\mathrm{inel}}(n)}{I_{\mathrm{el}}} = \frac{p(n)(2-2j_0)}{5+4j_0+3M}$ which below will be compared to the experiment. If a tunnel splitting is not resolved the related inelastic transition is included in the elastic line with an obvious modification of the outlined equation.

The correspondence principle requires a smooth transition from tunnelling characterized by inelastic transitions to classical jump reorientation characterized by quasielastic spectra with increasing the sample temperature. A perturbational calculation [18] shows that the tunnel transitions shift by $\Delta\hbar\omega_t$ towards the elastic line and broaden by $\Gamma_{t_n}(T)$ temperature

$$\begin{aligned} \Delta\hbar\omega_{t_n}(T) &\sim \exp(-E_{S_n}/kT) \\ \Gamma_{t_n}(T) &= \Gamma_{0_n}\exp(-E_{\Gamma_n}/kT). \end{aligned} \tag{4}$$

The theory shows that the activation energy E_{Γ_n} represents E_{01}^n, the librational energy of the nth methyl group, and $E_{S_n} \leqslant E_{01}^n$.

Stochastic reorientational jumps at higher temperatures lead to quasielastic scattering. Classical jump reorientation is characterized by a jump time τ and the corresponding jump rate $\tau^{-1} \sim \Gamma(T)$ which for large barriers obeys an Arrhenius function with a characteristic

activation energy E_a. E_a is calculated from equations (2) and (1) as the distance of the potential maximum from the ground state energy E_0. In the case of N inequivalent methyl groups and M immobile protons the neutron scattering function is [19]

$$\begin{aligned} S(Q,\omega) &= (1+2j_0(Qd)+M)\delta(\omega)+\sum_{n=1}^{N} p(n)2(1-j_0(Qd))L(\Gamma_n,\omega) \\ L(\Gamma_n,\omega) &= \frac{1}{\pi}\frac{\Gamma_n}{\Gamma_n^2+\omega^2} \\ \Gamma_n(T) &= \Gamma_{0_n}\exp(-E_{a_n}/kT). \end{aligned} \tag{5}$$

Here the jump distance d is—as above—given by the proton–proton distance of the methyl group. Some Lorentzians may collapse into a single line if their widths Γ_n are not different enough to be resolved.

3. Sample preparation and characterization

The dark-pink crystals of the TMP–CLA 1:1 complex were grown from acetone. The monoclinic structure determined at 100 K by x-ray diffraction [10] shows space group $P2_1/c$ with $Z = 2$ dimers in the unit cell. Due to symmetry the two units are equivalent. The irreducible unit of tetramethylpyrazine is finally half a molecule due to a centre of inversion. This reduces the number of inequivalent methyl groups to two (figure 1). However, the x-ray and neutron diffraction studies performed at 14 K [17] show the space group $P2_1/n$ with $Z = 4$ dimers in the unit cell due to a doubling of the unit cell along the a axis. The most important difference between the 14 and 100 K structures consists in a slightly different geometry of hydrogen bonds. While in the 100 K packing there is one type of infinite hydrogen bonded chains with an O·H···N bridge length equal to 2.692(2) Å and the O·H···N angle equal to 161(3)° there are two alternating types of hydrogen bonds in the chain with R_1(O·H···N) = 2.668(1) Å and the angle α_1(O·H···N) = 156.8(2)° and with R_2(O·H···N) = 2.713(1) Å and the angle α_2(O·H···N) = 156.6(2)° at a temperature $T = 14$ K. This implies four types of methyl groups in the TMP–CLA crystal at the lowest temperatures.

4. Spectroscopic results and discussion

4.1. Methyl rotational tunnelling and crystal structure implications

The backscattering spectrometer BSS of Forschungszentrum Jülich [20] was used with its SiGe offset monochromator. This set-up gives access to energy transfers $-32 \leqslant \hbar\omega[\mu\text{eV}] \leqslant 3$ at an energy resolution $\delta E_{\text{res}} = 1.9$ μeV. A flat sample holder of 1 mm thickness was filled with the powdered polycrystalline material and oriented under −45° to the neutron beam. Thus the large momentum transfer angles which show the strongest signal are used in reflection geometry.

At helium temperature three sharp tunnelling modes at energies 3.3, 20.6 and 28.5 μeV of relative intensities 4:1:2.5 are observed (figure 2). For low momentum transfers the integrated inelastic intensities and the elastic intensity show almost exactly the intensity ratio calculated from equation (3). This means that the tunnelling splittings of all methyl groups of TMP are resolved. At larger momentum transfers the ratio is reduced due to contamination of the elastic intensity by low Q Bragg scattering from a large unit cell.

For a unit cell determined at $T = 14$ K [17] we would expect four equally intense tunnelling peaks attributed to four types of methyl groups with different environments. This is not observed. A part of the inconsistency can be removed by assigning the tunnel band

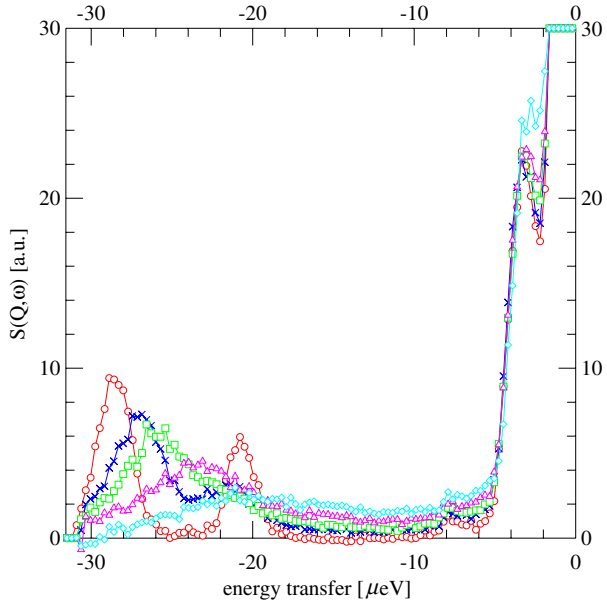

Figure 2. Temperature dependence of the tunnelling spectra of the TMP–CLA 1:1 complex. A smooth evolution of spectra from a sample temperature $T = 4.58$ K (○) via 17 K (×), 19 K (□), 22 K (△) to $T = 25.94$ K (◇) is observed. Spectrometer: BSS of FZJ. Wavelength $\lambda = 6.27$ Å. Average momentum transfer $Q = 1.6$ Å^{-1}.

at 3.0 μeV to two overlapping lines. However, the two well resolved bands at high energy transfers show different intensities in disagreement with the equal occurrence probabilities $p(n)$ deduced from the structure. If there were another phase transition at further cooling of the material below $T = 14$ K, for example by another doubling of the unit cell along the c axis, then one could explain the intensity of the weakest band. At the same time many accidental degeneracies are required. This is not very convincing, either. On the other hand, the unusual shift of the line at 20.59 μeV towards larger energies with increasing temperature leads to merging of the two high energy tunnel modes. Due to this behaviour fits above $T \sim 21$ K can identify two modes of similar intensities. This spectrum looks as expected for the high temperature crystal structure of the complex [10].

The temperature evolution of the positions and widths of tunnelling lines is shown in figure 3. The shift of the tunnelling peak at 28.53 μeV with temperature is shown in figure 4 in an Arrhenius presentation. The fit (solid line) gives an activation energy $E_{S_3} = 9.2$ meV; see equation (4). This value should be equal to or smaller than the energy of the librational mode of this methyl group. A similar evaluation for the inner tunnelling line at $\hbar\omega_t = 3.3$ μeV yields $E_{S_1} = 13.9$ meV. These values are rather close to the two main peaks of the vibrational density of states VDOS of TMP–CLA and confirm their assignment to methyl librational modes. Only this temperature dependence allows us to attribute a specific librational band from the many observed to a specific tunnelling mode. This correlation is used below when deriving rotational potentials.

A less specific technique to study the dynamics of a material is to measure the purely elastic scattering as a function of sample temperature. When the width Γ of the quasielastic component due to the stochastic dynamical processes as described by equation (5) reaches the instrumental resolution with increasing temperature, intensity is lost from the energy window integrated by

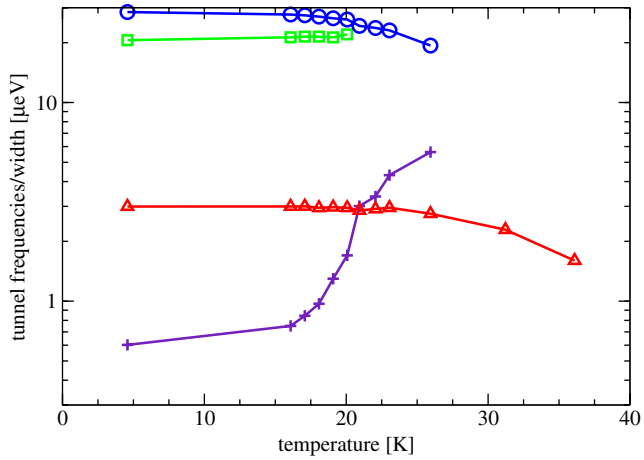

Figure 3. Temperature dependence of tunnel frequencies (○, □, △) and linewidth (+) of the band with the largest splitting $\hbar\omega_t = 28.5$ μeV of the TMP–CLA acid 1:1 complex.

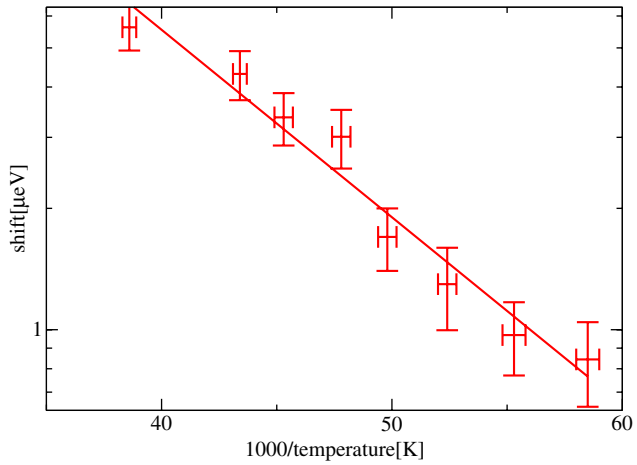

Figure 4. Arrhenius plot of the shift of the tunnelling peak at 28.53 μeV.

the resolution function. Theory shows that the elastic intensity should decrease according to a tanh-curve. Figure 5 represents the fixed-window spectrum for TMP–CLA for different momentum transfers. The characteristic temperature of the inclination point of the tanh-curve is $T_{1/2} \sim 45$ K. At this temperature the quasielastic linewidth is equal to the instrumental energy resolution of $\Gamma_{\text{res}} = 1.9$ μeV. From this value and an approximate value $\Gamma_0 = 4$ meV of the prefactor of the Arrhenius law, characterizing the attempt frequency, an activation energy of $E_{\text{a}} = 32$ meV can be estimated from the expression $E_{\text{a}} = \ln(\Gamma_0/\Gamma_{\text{res}}) * T_{1/2}$. For a pure $\cos(3\varphi)$ potential this activation energy is connected with a tunnel splitting of 3.2 μeV which agrees well with the low energy tunnel splitting observed. Beside of the discussed process the fixed-window scan (figure 5) contains the features of all other dynamical processes. If we estimate $T_{1/2}$ for the methyl group rotation connected with the tunnel splitting of $\hbar\omega_t = 28.5$ μeV assuming again a $\cos(3\varphi)$ potential we obtain $T_{1/2} \sim 24$ K. This means that the two processes cannot be clearly separated by the fixed-window method.

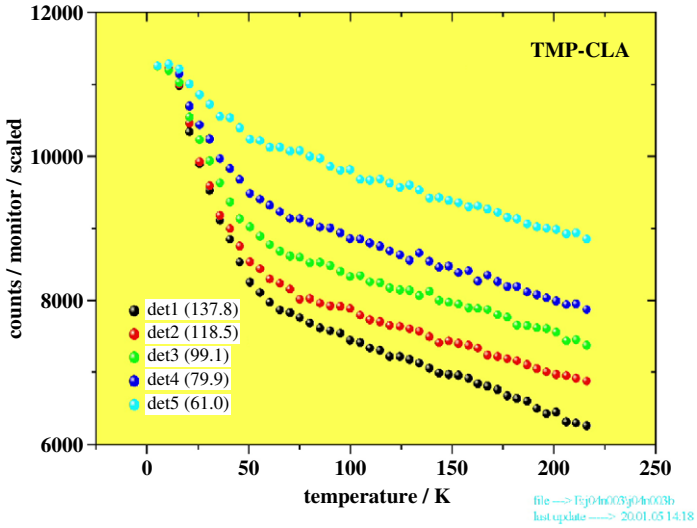

Figure 5. Temperature dependence of the elastic intensity (fixed-window scan) of the TMP–CLA 1:1 complex. Spectrometer: BSS of FZJ. Wavelength $\lambda = 6.27$ Å. The intensity step marks the onset of classical dynamics. The step height increases with momentum transfer according to equations (3) and (5). Top line: $Q = 1.00$ Å^{-1}. Bottom line: $Q = 1.82$ Å^{-1}.

The intensity step increases with momentum transfer. For the lowest momentum transfer the observed decrease is very close to the ratio one gets if the total elastic intensity at low temperature, $T = 4.58$ K, is calculated from the scattering function equation (3) and at high temperature, $T \geqslant 70$ K, from the scattering function equation (5) with the assumption that all tunnelling bands are resolved. With increasing momentum transfer the intensity loss becomes lower than expected theoretically likely due to coherent scattering which contaminates the elastic line. (For unresolved tunnel splittings the intensity drop at $T_{1/2}$ is about a factor of three larger according to equation (5).)

There is no discontinuity in the change of intensity which could be correlated to the phase transition at $T_c \sim 95$ K. Since all quasielastic intensity is already outside of the elastic window the incoherent elastic intensity can only be sensitive to a phase transformation which increases significantly the rotational barriers to bring quasielastic intensity back into the elastic line. Since this is not observed the rotational barriers in the high temperature phase are likely weaker than in the low temperature phase.

The link to methyl librational energies $\hbar\omega = E_{01}$ can be made by assigning the loss of elastic intensity to Debye–Waller factor fully due to a methyl librational mode

$$I(Q,T) = I_0 * \exp(-\tfrac{1}{3}\langle u(T)^2\rangle Q^2). \tag{6}$$

From this equation and the equipartition principle $\frac{1}{2}m\langle u^2\rangle\omega^2 = \frac{1}{2}kT$ and inserting three proton masses for m we get

$$E_{01} = 0.24Q\sqrt{\frac{T}{\ln\frac{I_0}{I(Q,T)}}} \tag{7}$$

with momentum transfer Q taken in units Å^{-1} and temperature T in Kelvin. The two Q-dependent terms in this equation nearly cancel and the librational energy is independent of momentum transfer as it should be. With the values from the experiment an average librational

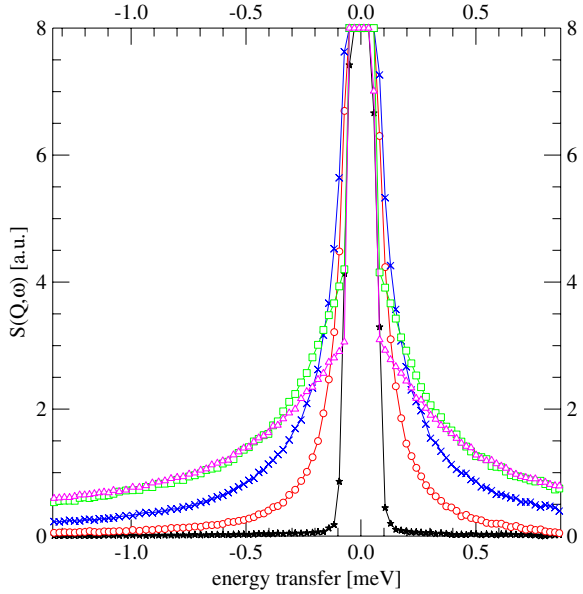

Figure 6. Temperature dependence of quasielastic spectra of the TMP–CLA 1:1 complex. Sample temperatures $T = 41.3$ K (○), 58.0 K (×), 118 K (□), 138 K (△). Resolution function (⋆). Spectrometer: IN5 of ILL. Wavelength $\lambda = 6.5$ Å. Average momentum transfer $Q = 1.6$ Å^{-1}.

energy $E_{01} \sim 10$ meV is obtained, which fits well to the two librational bands found in the VDOS at 8 and 14 meV.

4.2. Methyl rotational barriers and quasielastic scattering

The improved cold time-of-flight spectrometer IN5 at the Institut Laue–Langevin [21] was used at a wavelength $\lambda = 6.5$ Å to measure stochastic reorientational processes by quasielastic neutron scattering. The same sample which was used in the high resolution backscattering experiment was measured at identical orientation of the sample.

The fit by two Lorentzians of equal intensities is almost perfect in the whole temperature regime. The smooth broadening follows Arrhenius behaviour (figure 7) with activation energies shown in table 2. The transition into the high temperature phase, observed at $T = 95$ K, seems not to affect the rotational barriers measurably. We will discuss the activation energies of the two weakly hindered inequivalent methyl groups when constructing rotational potentials below.

4.3. Methyl librations and vibrational density of states

The spectra of TMP and TMP–CLA in the regime of phonons were measured using the spectrometer SV29 of Forschungszentrum Jülich [20] at wavelengths $\lambda = 1.76$ and 1.81 Å. The identical sample used on the other spectrometers was used oriented under an angle of $-45°$.

The phonon spectra obtained at direct time-of-flight spectrometer SV29 at the continuous neutron source DIDO in Jülich for low energy transfer (figures 8 and 9) are confirmed by spectra from the NERA-PR inverse time-of-flight spectrometer [22] at the pulsed reactor IBR-2 in Dubna (figure 10). These latter spectra range up to much higher energy transfers, up to 150 meV.

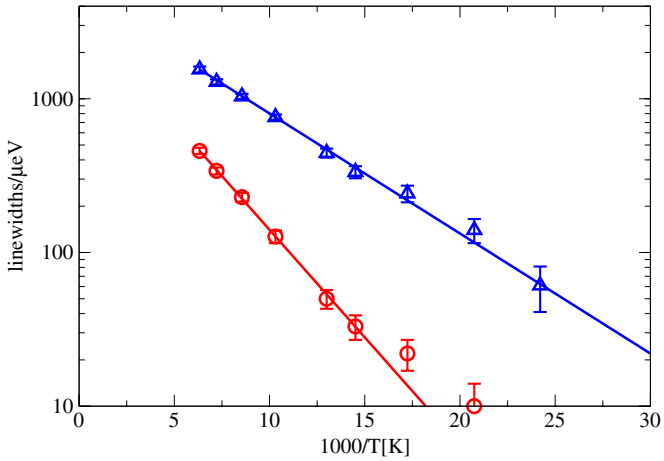

Figure 7. Quasielastic linewidths extracted from spectra of figure 6. The uncertainty is given by systematic errors. Solid lines represent Arrhenius fits. Activation energies are shown in table 2.

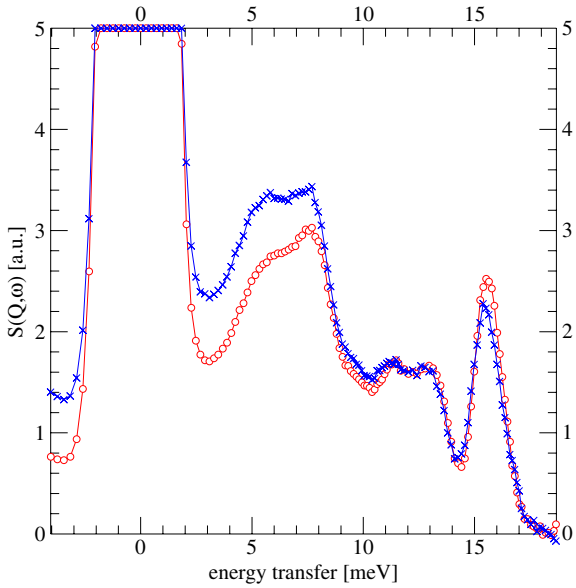

Figure 8. Spectrum of pure TMP in the regime of phonon energies. Sample temperatures $T = 2.4$ K (O) and 46 K (×). Spectrometer: SV29 of FZJ. Wavelength $\lambda = 1.76$ Å. Average momentum transfer $Q = 4.2$ Å^{-1}.

Different analytical concepts have to be used to describe the excitation bands at different regimes of energy transfer as explained below.

The internal modes at high energy transfers are little affected by the aggregation in the solid state due to the weakness of van der Waals forces. Therefore theoretical chemistry programs developed for single molecules are well suited to describe these modes. The harmonic force field for an isolated tetramethylpyrazine molecule was calculated after geometry optimization using the B3LYP model at the 6-311G (d, p) level as implemented in the GAUSSIAN 98 package [23]. The potential energy distributions for normal modes were calculated using the

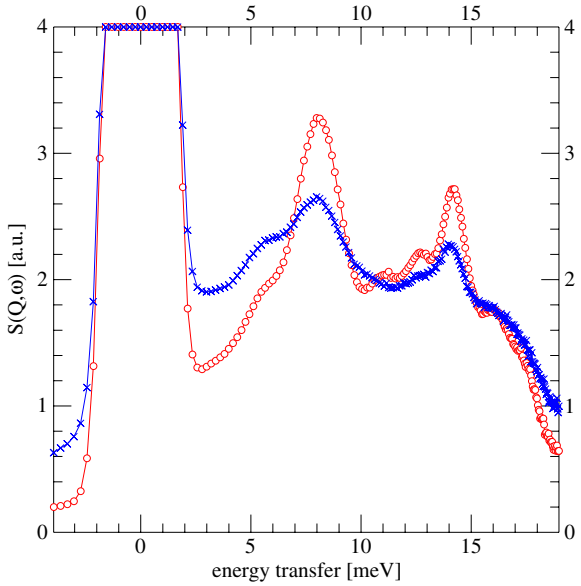

Figure 9. Spectrum of the TMP–CLA 1:1 complex in the regime of phonons. Sample temperatures $T = 2.4$ K (○) and 46 K (×). Spectrometer: SV29 of FZJ. Wavelength $\lambda = 1.81$ Å. Average momentum transfer $Q = 4.0$ Å^{-1}.

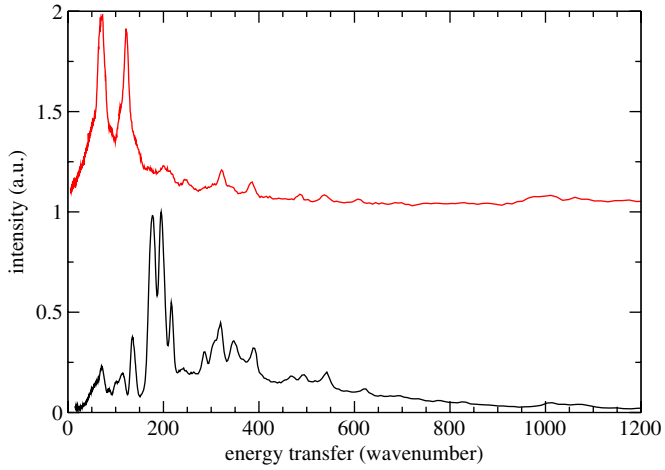

Figure 10. Density of states of pure TMP (bottom) and TMP–CLA (top) as measured with the NERA-PR spectrometer at the pulsed reactor IBR-2. Sample temperatures $T = 20$ K. (0.04 cm^{-1} = 1 meV.)

GAMESS program [24] on the B3LYP/6-31G(d, p) level. The corresponding modes were defined by means of internal coordinates according to Pulay *et al* [25]. Table 1 shows the comparison of the calculated eigenmode energies of the isolated TMP molecule with the measured transition energies. A reasonable agreement is obtained for internal modes above energies of about 240 cm^{-1} (30 meV). At lower energies the intermolecular interaction begins to play an important role and the good agreement is lost. The influence of the environment is

Table 1. Comparison of the measured energy bands of pure TMP and TMP–CLA 1:1 complex with GAUSSIAN calculation of the internal modes of the isolated TMP molecule. Energies in cm^{-1}. 1 meV = 8.04 cm^{-1}.

Approximate assignments	Calculated[a] B3LYP/6-31G**	Experimental INS	
		TMP	TMP*CLA
Long. acoust. ph.		44	44
Trans. acoust. ph.		62	66
Optical phonon		92	88
Optical phonon		105	103
Optical phonon			129
Ring torsion	91	130	110
CH_3 tors.	120	171	68
CH_3 tors.	122	171	74
CH_3 tors.	140	190	122
CH_3 tors.	156	190	124
Overtone (2 × 68, 2 × 74)			141
Combination (68 + 122, 68 + 124, 74 + 122, 74 + 124)			196
Ring torsion	196	211	209
Overtone (2 × 122, 2 × 124)			245
Ring torsion	274		
C–CH_3 bend.	282	280	288
C–CH_3 bend.	303	300	305
C–CH_3 bend.	303	313	322
C–CH_3 wagg.	381	382	385
C–CH_3 wagg.	476	463	480
Ring def.	486	491	486
C–CH_3 bend.	531	536	537
Ring def.	537	543	543
C–CH_3 wagg.	617	616	609
C–CH_3 str.	680	688	691
C–N str.	727	736	
C–CH_3 wagg.	775	775	
C–CH_3 str.	820	824	830
CH_3 rock.	991		977
CH_3 rock.	1002		
CH_3 rock.	1013	1005	1010
CH_3 rock.	1028		
CH_3 rock.	1051		
CH_3 rock.	1069	1068	1062
CH_3 rock.	1070		
CH_3 rock.	1080		
C–CH_3 str.	1131	1144	1151
Ring def.	1238	1196	1175

[a] No scaled frequencies, calculated for isolated TMP molecule.

obvious when comparing the measured spectra of TMP and TMP–CLA. The same molecule, TMP, in two different compounds shows completely different eigenmodes and phonon spectra.

Already an isolated TMP molecule shows a complex low frequency spectrum. The presence of four methyl groups implies the presence of four energetically different eigenmodes of predominantly CH_3 librational character due to the four possible in- and out-of-phase motions of neighbouring groups. In the solid state the environment of TMP reduces the molecular symmetry. Above $T = 110$ K the crystal structure of pure TMP is *Pbca*,

Table 2. TMP: rotational potentials obtained from the librational energies. TMP–CLA: rotational potentials adjusted for the **bold** values, (a) $\hbar\omega_t$ and E_a, (b) $\hbar\omega_t$ and E_{01}. Values in brackets are calculated.

Sample	Potential V_3 (meV)	Potential V_6 (meV)	$\hbar\omega_t$ (μeV)	E_{01} (meV)	E_a (meV)
TMP	95.0		(0.02)	**22.0**	(84)
	108.0		(0.001)	**23.6**	(96)
TMP–CLA	37.0	4.0	**3.3**	**14.6**	28.9
a	21.6	5.0	**20.9**	11.0	**14.7**
b	29.7	−9.0	**20.6**	**8.4**	26.6
a	21.0	2.0	**28.8**	9.9	**15.2**
b	25.4	−6.0	**28.6**	**8.4**	21.8

$Z = 4$ [8]. An inversion centre at the site of the molecule distributes the methyl groups into two crystallographically distinct pairs. While one of these pairs is involved in C–H $\cdots$ N bonds to a neighbour molecule the second pair approaches in close packing methyl groups of another neighbour [9] (figure 1). This symmetry reduction complicates the eigenmode spectrum. A quantitative description has finally to include the translations and rotations of the whole molecule in the potential of its neighbours. To reproduce all phonon energies requires a full lattice dynamical calculation on the basis of an accurate knowledge of the crystal structure and reasonable intermolecular interaction potentials. In the absence of such knowledge or a too high complexity of the mathematical problem a qualitative understanding can be obtained by modeling the essential structural and dynamical features of a compound. This is the way the CLIMAX program [26] works. AuntieCLIMAX is a modified PC version of the CLIMAX program adapted to parameters of the NERA-PR spectrometer. A CLIMAX calculation includes overtones, combination lines and phonon wings which are most often taken from the measured data. Due to input from the measured data spectra can be described *semiquantitatively*.

The experiment (figure 10, bottom) shows that for pure TMP the scattered intensity is concentrated in two bands. We tentatively assign these two dominant bands at 22.0 and 23.6 meV to modes of predominantly methyl librational character. Led by the symmetry of the modes in the isolated molecule we assign the lower energy band to modes with out-of-phase, the higher one to modes with in-phase, rotation of neighbouring groups.

Compared to the pure compound the complexation with CLA changes the nearest environment of TMP completely (figure 1). This severe change seems not very much to modify the dynamics of the molecule as a whole. The acoustic phonons still appear at (5–8) meV. The band at 8.2 meV has strongly increased in intensity (figure 10, top, figure 9), however. This and the second intense band at 15.6 meV, lying in the regime of lattice modes, are assigned to the two groups of energetically different methyl librational eigenmodes of two crystallographically independent [10] pairs of methyl groups. The fast damping of these modes with increasing sample temperature supports this assignment. The widths of the two bands may in part be due to dispersion but also in part to a splitting into close subbands due to the symmetry reduction in the low temperature crystal structure [17]. In agreement with the separation of tunnelling into roughly two bands the differences between each two types of methyl potentials is small. By assigning the two strong low energy bands to methyl librations the main features of the spectrum are well reproduced by the auntieCLIMAX program based on calculated mass weighted normal vibrational coordinates (figure 11). Overtones etc are indicated in the figure and included in the mode assignment presented in table 1.

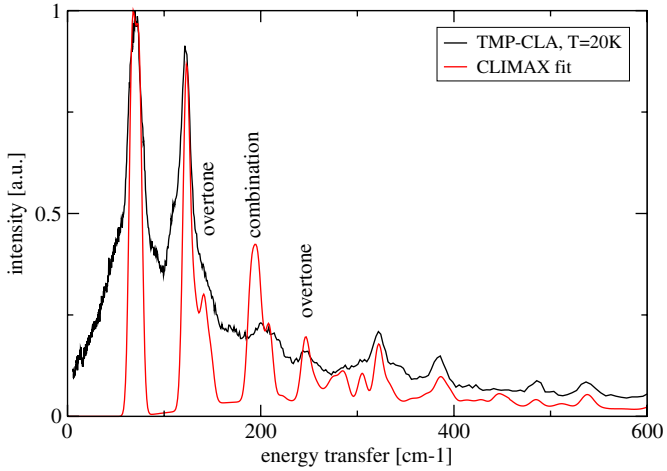

Figure 11. Density of states of TMP–CLA. Sample temperatures $T = 20$ K The solid line is a fit using the auntieCLIMAX program. The model is based on two inequivalent methyl librational modes represented by the two strong low energy modes.

4.4. Rotational potentials

In the case of TMP the determination of rotational potentials is based on librational modes only. The $\cos(3\varphi)$ potential then predicts the bracketed values of tunnel splittings and activation energies of table 2, rows 1 and 2. For TMP–CLA librational and tunnelling modes are observed and the rotational potential has to describe them consistently. Table 2, rows 3 and 4, shows that such a potential can be found for the strongly hindered methyl groups by adding about 10% of a sixfold to the leading threefold term.

For the two weakly hindered methyl groups we could not describe all three properties $\hbar\omega_t$, E_{01} and E_a simultaneously. There are two possible solutions. (a) The error can be attributed to a wrong interpretation of the librational mode E_{01}. For weak potentials librational modes couple to other external modes. The single-particle librational energies are averages of dispersed librational branches and not identical to peaks of the VDOS. A prominent example of this type is 2-butyne [27]. This view is supported by the activation energy $E_S = 9.2$ meV derived from the shift of the tunnel peak $\hbar\omega_{t3} = 28.6\,\mu$eV. According to theory [18] E_S should be close to the single-particle librational energy. (b) We distrust the activation energy since it is derived in a different temperature range and the sample is known to undergo phase transitions. At this condition a higher barrier to rotation E_a is calculated for the lowest temperature phase.

A comparison shows that on average the methyl rotational potentials in the TMP–CLA complex are weaker, in pure TMP stronger, than in the isolated molecule. This means that intermolecular interaction strongly influences the rotational potential. Whether hydrogen bond formation between the acid protons and the nitrogen atoms of TMP—including charge transfer—is important or whether only a change of steric hindrance and Coulomb interaction determine these changes cannot be decided without mathematical modelling [4]. Such an analysis will be the topic of a forthcoming publication.

5. Conclusion

The dynamics of tetramethylpyrazine (TMP) in the 1:1 complex with chloranilic acid was studied with special emphasis on methyl group rotation and compared to pure TMP. The

vibrational density of states is interpreted by a GAUSSIAN 98 analysis with respect to internal vibrations and by CLIMAX modelling with respect to methyl librational modes. In the case of the TMP–CLA complex methyl rotational tunnelling splittings could be resolved and rotational barriers obtained from quasielastic neutron spectra. The number and intensities of tunnelling peaks are compared to the predictions of the crystal structure [17]. While the number of transitions estimated under the assumption that the strongest line at 3.3 μeV represents two accidentally degenerate rotor systems agrees with the number of inequivalent methyl groups of the crystal structure their intensities differ somewhat from the occurrence probabilities. This discrepancy is a sign of an incomplete understanding of the crystal structure. A new structure refinement is needed as the basis of future mathematical modelling. Rotational potentials are derived which fit the tunnelling splittings and librational energies of methyl groups in TMP–CLA. While the calculated activation energies calculated for the more hindered methyl groups fit well with the one obtained from quasielastic scattering, they are significantly too low for the weakly hindered rotors. This discrepancy is attributed to the unknown phase behaviour of the material since E_a is determined in a different temperature regime. Methyl librational modes in pure TMP are connected with stronger rotational potentials as in the complex. Potentials calculated for the isolated molecule using the GAUSSIAN 98 program package are stronger than in TMP–CLA but weaker than in TMP. Two effects influence the rotational potential, the change of the neighbourhood (packing effects) and the change of the charge distribution in the dimer by either charge transfer or the formation of hydrogen bonds. To quantify these contributions precise lattice dynamical calculations including the determination of methyl rotational potential are necessary for the pure material and the complex. Earlier work on pure molecular systems has shown [28] that in hydrogen bonded materials consistency cannot be obtained without allowing a rearrangement of charges. A new crystal structure determination is needed to get the basis for such mathematical modelling.

Acknowledgments

We thank the Institut Laue–Langevin, Grenoble, for test beamtime to measure quasielastic spectra and Stefan Mattauch from FZJ for helpful discussions and communication of unpublished results of the low temperature crystal structure. Support from the Polish Ministry of Science and Informatics (grant 4T09A 05125) is acknowledged. This research project has also been supported by the European Commission under the Sixth Framework Programme through the Key Action 'Strengthening the European research area, research infrastructures', contract RII3-CT-2003-505925.

References

[1] Press W 1981 *Single Particle Rotations in Molecular Crystals* (*Springer Tracts in Modern Physics* vol 81) (Berlin: Springer)
[2] Prager M and Heidemann A 1997 *Chem. Rev.* **97** 2933
[3] Prager M, David W I F and Ibberson R M 1991 *J. Chem. Phys.* **95** 2473
[4] Johnson M R and Kearley G J 2000 *Annu. Rev. Chem.* **51** 297
[5] Plazanet M, Johnson M R, Gale J D, Yildirim T, Kearley G J, Fernandez-Diaz M T, Sanchez-Portal D, Artacho E, Soler J M, Ordejon P, Garcia A and Trommsdorff H P 2000 *Chem. Phys.* **261** 189
[6] Neumann M A, Johnson M R, Radealli P G and Trommsdorff H P 1999 *J. Chem. Phys.* **110** 516
[7] Pawlukojc A and Sobczyk L 2005 *Trends Appl. Spectrosc.* at press
[8] Braam A W M, Eshuis A and Vos A 1981 *Acta Crystallogr.* B **37** 730
[9] Thalladi V R, Gehrke A and Boese R 2000 *New J. Chem.* **24** 463

[10] Sawka-Dobrowolska W, Bator G, Sobczyk L, Grech E, Nowicka-Scheibe J and Pawlukojc A 2005 *Struct. Chem.* at press
[11] Zaman Md B, Tomura M and Yamashita Y 1999 *Chem. Commun.* 999
Zaman Md B, Tomura M and Yamashita Y 2000 *Org. Lett.* **2** 273
Zaman Md B, Tomura M and Yamashita Y 2001 *J. Org. Chem.* **66** 5987
[12] Trimpower B L (ed) 1982 *Functions of Quinones in Energy Converting Systems* (New York: Academic)
[13] Clinman J P and David M 1994 *Annu. Rev. Biochem.* **63** 299
[14] Ishida H and Kashino S 1999 *Acta Crystallogr.* C **55** 1149
[15] Ishida H and Kashino S 2004 *Acta Crystallogr.* C **57** 476
[16] Ishida H and Kashino S 1999 *Acta Crystallogr.* C **55** 1714
[17] Pietraszko A and Mattauch S, unpublished; thanks are to authors for permission to use their data before publishing
[18] Hewson A C 1982 *J. Phys. C: Solid State Phys.* **15** 3841
Hewson A C 1982 *J. Phys. C: Solid State Phys.* **15** 3855
[19] Bée M 1988 *Quasielastic Neutron Scattering* (Bristol: Hilger)
[20] http://www.fz-juelich.de/iff/Institute/ins/Broschuere_NSE/
[21] http://www.ill.fr/YellowBook/IN5/
[22] Natkaniec I, Bragin S I, Brankowski J and Mayer J 1993 *Proc. ICANS-XIII (Abingdon) RAL Report* 94-025 vol 1, p 89
[23] Frisch M J *et al* 1998 *Gaussian 98, Rev. A.9 Programme* (Pittsburgh, PA: Gaussian)
[24] Schmidt M W, Baldrige K K, Boatz J A, Elbert S T, Gordon M S, Jensen J H, Koseki S, Matsunaga N, Nguyen K A, Su S J, Windens T L, Depois M and Montgomery J A 1993 *J. Comput. Chem.* **14** 1347
[25] Pulay P, Fergasi G, Pang F and Boggs J E 1979 *J. Am. Chem. Soc.* **101** 2550
[26] Tomkinson J, Ramirez-Cuesta A J, Champion W, Lawrence J W and Parker S F *auntieCLIMAX, a users guide*
[27] Kirstein O, Prager M, Johnson M R and Parker S F 2002 *Appl. Phys.* A **74** 1323
[28] Johnson M, Prager M, Grimm H, Neumann M A, Kearley G J and Wilson C C 1999 *Chem. Phys.* **244** 49